JPET Fast Forward. Published on December 17, 2004 as DOI: 10.1124/jpet.104.078469

JPET #78469

<u>Full Title:</u> Protein Kinase C Delta (PKCδ) is a Key Downstream Mediator of Manganese-induced Apoptosis in Dopaminergic Neuronal Cells

Authors: Calivarathan Latchoumycandane, Vellareddy Anantharam, Masashi Kitazawa, Yongjie Yang, Arthi Kanthasamy and Anumantha G. Kanthasamy*

Institution: Parkinson's Disorder Research Laboratory, Department of Biomedical Sciences, Iowa State University, Ames, IA 50011-1250, USA

Running Title: Proteolytic activation of PKCdelta in apoptosis

*Correspondence to: Dr. A.G. Kanthasamy, Parkinson's Disorder Research Laboratory, Department of Biomedical Sciences, 2008 Veterinary Medicine Building, Iowa State University, Ames, IA 50011-1250; Phone: (515) 294-2516; Fax: (515) 294-2315; e-mail: akanthas@iastate.edu

Text Pages: 37

Tables: 0

Figures: 10

References: 40/40

Abstract: 235/250 words

Introduction: 281/750 words

Discussion: 1488/1500 words

Abbreviations: ELISA, Enzyme-Linked Immuno-sorbent Assay; GFP, Green Fluorescence Protein; MMT, Methylcyclopentadienyl Manganese Tricarbonyl; MPP^+, 1-Methyl-4-PhenylPyridinium; MTT, 3-(4,5-dimethylthiazol-2-yl)-2,5-diphenyltetrazodium bromide; PC12, rat Pheochromocytoma Cells; $PKC\delta^{D327A}$, Protein Kinase Cdelta-Cleavage Resistant Mutant; $PKC\delta^{K376R}$, Protein Kinase Cdelta-Dominant Negative Mutant; PKC, Protein Kinase C; RNAi, Ribonucleic Acid Interference; ROS, Reactive Oxygen Species; siRNA, small Interfering Ribonucleic Acid; Z-DEVD-FMK, Benzyloxycarbonyl-Asp-Glu-Val-Asp-Fluoromethylketone; Z-VAD-FMK, Benzyloxycarbonyl-Val-Ala-Asp-Fluoromethylketone.

Recommended Section: Toxicology

ABSTRACT

Manganese (Mn) exposure causes Manganism, a neurological disorder similar to Parkinson's disease. However, the cellular mechanism by which Mn induces dopaminergic neuronal cell death remains unclear. In the present study, we sought to investigate the key downstream apoptotic cell signaling events that contribute to Mn-induced cell death in mesencephalic dopaminergic neuronal (N27) cells. Mn exposure induced a dose-dependent increase in neuronal cell death in N27 cells. The cell death was accompanied by sequential activation of mitochondrial-dependent proapoptotic events including cytochrome c release, caspase-3 activation, and DNA fragmentation, but not caspase-8 activation, indicating that the mitochondrial-dependent apoptotic cascade primarily triggers Mn-induced apoptosis. Notably, Mn treatment proteolytically activated protein kinase Cδ (PKCδ), a member of a novel class of protein kinase C. The caspase-3 specific inhibitor Z-DEVD-FMK significantly blocked PKCδ cleavage and its kinase activity, indicating that caspase-3 mediates the proteolytic activation. Co-treatment with the PKCδ inhibitor rottlerin or the caspase-3 inhibitor Z-DEVD-FMK almost completely blocked Mn-induced DNA fragmentation. Additionally, N27 cells expressing a catalytically inactive PKCδ^{K376R} protein (PKCδ dominant negative mutant) or a caspase cleavage resistant PKCδ^{D327A} protein (PKCδ cleavage resistant mutant) were found to be resistant to Mn-induced apoptosis. To further establish the proapoptotic role of PKCδ, RNAi-mediated gene knockdown was performed. siRNA suppression of PKCδ expression protected N27 cells from Mn-induced apoptotic cell death. Collectively, these results suggest that caspase-3-dependent proteolytic activation of PKCδ plays a key role in Mn-induced apoptotic cell death.

INTRODUCTION

Exposure to high levels of Manganese (Mn) has been shown to cause a Parkinson's-like syndrome known as Manganism. Increased incidences of Manganism have been observed among miners and industrial welders as well as farmers exposed to Mn-based pesticides such as fungicides, Maneb (Mn ethylene-bis-dithiocarbamate), and Mancozeb (Mn Cu Zn ethylene-bis-dithiocarbamate) (Roth and Garrick, 2003; Dobson et al., 2004; Olanow, 2004). Adverse neurological effects of Mn also occurred in people who drank water containing high levels of Mn in Japan, Greece, and Australia and in abusers who used the Mn-containing compound Bazooka, a cocaine-based drug (Ensing, 1985). Several lines of evidence suggest that exposure to Mn or Mn-containing compounds induces a variety of cellular changes including glutathione (GSH) and dopamine depletion, increased oxidative stress, and impairment of energy metabolism and antioxidant systems (Anantharam et al., 2002). Recently, oxidative stress and apoptosis have been reported to play important roles in neurodegenerative processes including Parkinson's disease (PD) (Dauer and Przedborski, 2003; Dawson and Dawson, 2003; Jenner, 2003). Although several studies have demonstrated effects of Mn on neuronal cells, the mechanism of Mn-induced dopaminergic neurodegeneration remains unclear. Recently, we developed an in vitro model of dopaminergic neurotoxicity namely N27 cells which is derived from the mesencephalon, a brain region directly affected by PD. N27 cells also represent a homogenous population of dopaminergic tyrosine hydroxylase positive cells with functional characteristics, including cellular signaling, similar to dopaminergic neurons (Anantharam et al., 2002; Kaul et al., 2003). Using a combination of pharmacological inhibitors, RNAi-mediated gene knockdown, and

overexpression of PKCδ dominant negative and caspase resistant mutants, we herein demonstrated that caspase-3-mediated proteolytic activation of PKCδ plays a pivotal role in Mn-induced apoptosis in N27 mesencephalic dopaminergic cells.

MATERIALS AND METHODS

Materials. The immortalized rat mesencephalic dopaminergic neuronal cell line $1RB3AN_{27}$, normally referred to as N27 cells, was a kind gift from Dr. Kedar N. Prasad (University of Colorado Health Sciences Center, Denver, CO). Manganese chloride ($MnCl_2$, 99%), ATP, Protein-A-Sepharose, phosphatidylserine, dioleoylglycerol, and β-actin (mouse monoclonal) were obtained from Sigma (St. Louis, MO), rottlerin was purchased from Calbiochem (San Diego, CA), and Z-Asp-Glu-Val-Asp-fluoromethyl ketone (Z-DEVD-FMK) was obtained from Alexis Biochemicals (San Diego, CA). Acetyl-Asp-Glu-Val-Asp-7-amino-4-methylcoumarin (Ac-DEVD-AMC) was obtained from Bachem (King of Prussia, PA). Antibodies to PKCα, PKCβ, and PKCδ were purchased from Santa Cruz Biotechnology (Santa Cruz, CA), and the ECL chemiluminescence kit was purchased from Amersham Pharmacia Biotech (Piscataway, NJ). Hoechst 33342 and the Sytox Green Fluorescent Probe were purchased from Molecular Probes (Eugene, OR). Cell Death Detection ELISA Plus assay kit was purchased from Roche Molecular Biochemicals (Indianapolis, IN). [^{32}P]-γ-ATP was purchased from Perkin Elmer (Downers Grove, IL). Bradford protein assay reagent was purchased from Bio-Rad (Hercules, CA). RPMI-1640 medium, horse serum, fetal bovine serum, L-glutamine, penicillin, and streptomycin were purchased from Invitrogen (Gaithersburg, MD). Plasmids for pPKCδ^{K376R}-GFP and pEGFP-N1 were kind gifts from

Dr. Stuart Yuspa (National Cancer Institute, Bethesda, MD). PKCδ^{D327A}-GFP (PKCδ-CRM) construct was obtained from Dr. Mary Reyland's Laboratory at the University of Colorado (Boulder, CO).

Cell Culture. The immortalized rat mesencephalic cell line (N27 cells) was grown in RPMI-1640 media containing 10% fetal bovine serum, 2 mM L-glutamine, 50 units penicillin, and 50 μg/ml streptomycin (Kaul et al., 2003; Yang et al., 2004). The cell line was incubated at 37°C in a humidified atmosphere containing 5% CO_2.

Cytotoxicity Assays. The N27 cells were incubated with 10-5000 μM $MnCl_2$ for 24 hr and cell death was determined by MTT (3-(4,5-dimethylthiazol-3-yl)-2,5-diphenyl tetrazolium bromide) assay, which is widely used to assess cell viability (Kitazawa et al., 2001). After treatment with $MnCl_2$, the cells were incubated in serum-free medium containing 0.25 mg/ml MTT for 3 hr at 37°C. Formation of formazan from tetrazolium was measured at 570 nm with a reference wavelength at 630 nm using a SpectraMax microplate reader (Molecular Devices, Sunnyvale, CA). Cell death was also determined after exposing N27 cells to 100 μM or 300 μM $MnCl_2$ in the presence or absence of 50 μM Z-DEVD-FMK using the sytox green fluorescent based nucleic acid probe (Kaul et al., 2003). Sytox green is a cell-impermeable nucleic acid dye that enters dead cells and intercalates with DNA to produce green fluorescence, which was quantified using a fluorescence microplate reader (SpectraMax Gemini XS Model, Molecular Devices, Sunnyvale, CA) with excitation at 485 nm and emission at 538 nm.

Determination of Cytosolic Cytochrome C. Mn-induced cytochrome c release was measured using an ELISA kit as described previously (Kaul et al., 2003). Briefly, N27 cells (~5 x 10^6 cells) were exposed to 300 μM $MnCl_2$, cytoplasmic fractions were collected, and cytosolic cytochrome c levels were quantified colorimetrically by using a SpectraMax Gemini XS microplate reader.

Assay of Caspase-3 Activity. Caspase-3 activity was measured using a specific fluorescent substrate, Ac-DEVD-AMC, as described previously (Kaul et al., 2003). Briefly, cells (~1-2 x 10^5 cells/well) were subcultured in 24-well culture plates and treated with 100 μM or 300 μM $MnCl_2$ for 12 hr and 24 hr. Cells were lysed with lysis buffer containing 50 mM Tris/HCl (pH 7.4), 1 mM EDTA, 10 mM EGTA, and 10 μM digitonin. Lysates were then centrifuged at 10,000 x *g* for 5 min and cell-free supernatants were collected. Caspase-3 activity in the cell lysates was measured by incubating the caspase-3 specific fluorescent substrate Ac-DEVD-AMC (Kaul et al., 2003). Formation of 7-amino-4-methylcoumarine (AMC), resulting from caspase substrate cleavage, was measured using a SpectraMax Gemini XS microplate reader with excitation at 380 nm (slit width 10 nm) and emission at 460 nm (slit width 20 nm). Caspase activity was expressed as fluorescence units (FU)/mg protein/hr.

Determination of Proteolytic Cleavage of PKC Isoforms. N27 neuronal cells (~1 x 10^7 cells) were exposed to 100 μM or 300 μM $MnCl_2$ with or without the caspase-3 inhibitor Z-DEVD-FMK at 37°C for 24 hr, and cell lysates were prepared as described by Kaul et al., 2003. Briefly, N27 cells were washed with 1x phosphate buffered saline

(PBS), resuspended in homogenization buffer, and then sonicated for 10-15 sec. The homogenates from treated and control cells were centrifuged at 16,000 x *g* for 60 min at 4°C and the supernatants were collected as cell lysates. The lysates were mixed with 2X gel loading buffer containing 10% SDS and 200 mM DTT and placed in boiling water for 5 min. Proteins were resolved by 10-12% SDS-polyacrylamide gel electrophoresis (SDS-PAGE) and blotted onto nitrocellulose membrane (Bio-Rad Laboratories). After blocking the non-specific binding sites with 5% non-fat dry milk (Amersham Pharmacia Biotech), the membrane was then treated with anti-PKCδ (1:2000 dilution), anti-PKCα (1:1000), or anti-PKCβ (1:1000) antibodies, followed by secondary HRP-conjugated anti-rabbit (1:2000) antibody. Antibody-bound proteins were detected by an enhanced chemiluminescence (ECL) system using a Kodak Imager (Kodak Image Station 2000R, Eastman Kodak Company, New Haven, CT). To confirm equal protein in each lane, membranes were reprobed with β-actin (1:5000).

Assay of Protein Kinase Cδ Activity. PKCδ enzymatic activity was determined using immunoprecipitation as previously described (Kitazawa et al., 2003). The cells were exposed to 300 μM $MnCl_2$ for 24 hr, with or without a capase-3 inhibitor (Z-DEVD-FMK), and cell lysates were collected. After immunoprecipitation with anti-PKCδ antibody, 25 μl samples containing PKCδ bound to sepharose A beads were incubated with 25 μl of reaction buffer containing 0.4 mg histone H1 and 5 μCi of [γ-^{32}P] ATP (4,500 Ci/mM) for 10 min at 30°C. The reaction was terminated by the addition of 2X SDS gel loading buffer and boiled for 5 min. The samples were separated on 12.5% SDS-PAGE and histone phosphorylated bands were detected using a Phospho Imager

(Personal Molecular Imager FX, Bio-Rad Laboratories, Hercules, CA) and quantified using Quantity One 4.2.0 Software (Bio-Rad Laboratories).

Determination of DNA Fragmentation. DNA fragmentation was measured using a Cell Death Detection ELISA Plus Assay Kit (Roche Biochemical, IN), as previously described (Kitazawa et al., 2003). This highly sensitive assay for the detection of early apoptotic events measures the amount of histone-associated low molecular weight DNA in the cytoplasm of cells. Briefly, N27 cells were exposed to 300 μM $MnCl_2$ with or without 50 μM of the caspase-3 specific inhibitor Z-DEVD-FMK or 1-5 μM of the PKCδ specific inhibitor rottlerin for 24 hr. After treatment, cells were spun down, washed with 1X PBS, and incubated with cell lysis buffer (supplied with the kit) for 30 min at RT, and then centrifuged. The supernatants were then dispensed into streptavidin-coated 96 well microtiter plates containing 80 μl of HRP-conjugated antibody cocktail. After 2 hr incubation at RT, the nucleosomes retained by the antibody cocktail in the immunocomplex were quantified spectrophotometrically with ABTS as an HRP substrate. Measurements were made at 405 nm and 490 nm using a SpectroMax 190 spectrophotometer (Molecular Devices, Sunnyvale, CA). The difference of absorbance between OD 405 and OD 490 nm was used to measure the actual DNA fragmentation level.

Stable Transfection of PKCδ$^{K376\ R}$ Gene. Plasmid pPKCδ^{K376R}-GFP encodes protein kinase C-green fusion protein; K376R refers to the mutation of the lysine residue at position 376 to arginine in the catalytic site, which inactivates the PKCδ (Anantharam et

al., 2002). Plasmid pEGFP-N1 encodes the green fluorescent protein alone and is used as a vector control. N27 cells stably expressing PKCδ^{K376R}-GFP (herein referred to as PKCδ-DN cells) and GFP alone expressing cells (vector control) were cultured as described previously (Anantharam et al., 2002). The cells were exposed to 300 μM $MnCl_2$ for 24 hr and DNA fragmentation was measured as described above.

Lentiviral-mediated Transfection of Caspase Resistant PKCδ^{D327A} Mutant Gene. We used the ViraPower^{TM} Lentiviral Expression System (Invitrogen, Inc., Carlsbad, CA) to establish stable transfections of a caspase resistant mutant of PKCδ^{D327A} (aspartate to alanine mutation at position 327) into N27 cells (herein referred to as PKCδ-CRM). The PKCδ-CRM PCR fragment from pEGFP-N1 vector was subcloned into the plenti6/V5-D-TOPO expression vector, herein named plenti/PKCδ-CRM. Primers were: forward, 5'CACCATGGCACCCTTCCTGCTC3' and reverse, 5'AATGTCCAGGAATTGC TCAAAC3'. Standard cloning procedures were used. Lentiviral containing plenti6/PKCδ-CRM was produced by transfecting the plenti6/PKCδ-CRM construct into human 293FT cells using lipofectamine 2000 transfection reagent. The lentivirus in the medium was collected by centrifuging at 1500 x g for 15 min, 48-72 hr post-transfection. Lentiviral plenti/lacZ was also produced to serve as a vector control. Lentivirus containing plenti/PKCδ-CRM and polybrene (6 μg/ml) were added into cultured N27 cells (5 x 10^4). Stable cell lines were established by selection in 10 μg/ml blasticidin 48 hr after transfection. Colonies were isolated, then replated and grown to confluence in T75 flasks. Subsequently, the stable cell lines were maintained in 5 μg/ml blasticidin. PKCδ-CRM or lacZ expressing N27 cells were identified by immunostaining of the C-

terminal V5 epitope on expressed protein. After establishing a stable cell line, the cells were exposed to 300 μM $MnCl_2$ for 24 hr and DNA fragmentation was measured as described above.

PKCδ siRNA Experiments in N27 cells. PKCδ-siRNA was prepared by an in vitro transcription method as described previously (Yang et al., 2004). For this study, we synthesized a siRNA target site specific to rat PKCδ mRNA (gi: 18959249) and a non-specific siRNA (siRNA-NS). Template sequences of PKCδ-siRNA duplexes are 5'-AAAAGGCAAATTCACAAACA GCCTGTCTC-3' (forward) and 5'-AACTGTTTGTGAATTTGCCTTCCTGTCTC-3' (reverse) with the target site located at nucleotide 2142-2162 in rat PKCδ mRNA with a GC content of 47.6%. Template sequences of non-specific siRNA (siRNA-NS) duplexes are 5'-AAGTTCTCCGAAGTGTGAGAACCTGTCTC-3' (sense) and 5'-AATTCTCACAC TTCGGAGAACCCTGTCTC -3' (antisense). Previously, we showed that PKCδ-siRNA effectively suppresses >80% of PKCδ protein expression levels within 24 hr post-transfection (Yang et al., 2004). For siRNA, sense and antisense templates were chemically synthesized with a partial T7 promoter sequence. In vitro transcription, annealing, and purification of siRNA duplexes were performed as essentially as described previously (Yang et al., 2004). Synthesized and annealed siRNA duplexes were treated with DNase and RNase to remove the extra nucleotides of transcribed siRNA to meet the structural 3'UU overhang and 5'phosphate requirements before transfection experiments. N27 cells (50-70% confluency) were transfected with siRNA duplexes using a commercially available TKO transfection reagent (Mirus Corporation, Madison, WI).

Briefly, TKO reagent was diluted into RPMI 1640 medium for 15 min, and then the 25 nM siRNA duplex was added to form a lipid-siRNA complex. After an additional 15 min incubation, an siRNA-lipid transfection complex was added to the N27 cells cultured in 6-well plates. At 24 to 48 hr post-transfection, N27 cells were treated with 300 μM Mn for an additional 24 hr and used for the DNA fragmentation assay.

Data Analysis and Statistics. All the data were analyzed using Prism 3.0 Software (GraphPad Software, San Diego, CA). Data were first analyzed using one-way ANOVA, Dunnett's post-hoc test or Newman-Keuls test were performed to compare the differences between treatment groups. $p<0.05$ or less was considered significant.

RESULTS

Chronic Mn Exposure induces Dose-Dependent Increase in Cytotoxicity. In order to determine the optimal dose for a detailed mechanistic investigation, we first performed dose-response cytotoxicity analysis. A dose-dependent decrease in cell viability (Fig. 1A), as determined by MTT assay, was observed in N27 cells exposed to various concentrations of Mn. Exposure to 10 μM, 30, 100, 300, 1000, 3000, and 5000 μM Mn for 24 hr decreased the cell viability by 18%, 24%, 24%, 41%, 65%, 95%, and 97%, respectively, when compared to the control. An EC_{50} of 345 μM for Mn was deduced by three-parameter nonlinear regression. The dose-dependent effect of manganese on cell death was further quantified by Sytox green fluorescence assay. A 24 hr exposure to 100 μM and 300 μM Mn resulted in a 1-fold and 2-fold increase in Sytox green fluorescence,

respectively (Fig. 1B). Further, co-treatment with 50 μM Z-DEVD-FMK, a caspase-3 specific inhibitor, blocked more than 70% of 100 μM and over 74% of 300 μM Mn-induced cytotoxicity (Fig. 1B), suggesting that caspase-3 mainly mediates the Mn-induced cell death process in dopaminergic neuronal cells. Based upon these results, subsequent measurement of various biochemical indices in key mechanistic studies was performed in N27 cells treated with 300 μM Mn.

Mn Exposure Promotes Mitochondrial Cytochrome C Release. Several lines of evidence have recently shown that exposure to dopaminergic neurotoxins alters mitochondrial function, which can result in the release of a number of proapoptotic factors including cytochrome c and Smac/DIABLO into the cytosol (Kitazawa et al., 2001; Anantharam et al., 2002; Kaul et al., 2003) to initiate the apoptotic cascade. In the present study, treatment of N27 cells with 300 μM Mn resulted in a significant increase in cytosolic cytochrome c (Fig. 2) as compared to the control. Mn treatment increased cytosolic cytochrome c levels by 140% and 75% at 12 hr and 24 hr, respectively, as compared to the control.

Mn Induces a Dose- and Time-Dependent Activation of Caspase-3. Cytosolic cytochrome c is known to activate multiple caspases including caspase-9 and caspase-3 (Dawson and Dawson, 2003; Kanthasamy et al., 2003). Caspase-3 plays an important role in the execution of programmed cell death in both neuronal and non-neuronal cells. In the present study, we examined the effect of Mn on the activities of caspase-3 in N27 mesencephalic clonal cells. Exposure to Mn induced a time- and dose-dependent

increase in caspase-3 activity with respect to the control. Mn treatment at the concentrations of 100 μM and 300 μM induced 20% and 50% increases at 12 hr and 100% and 150% increases at 24 hr, respectively, as compared to the corresponding group of controls (Fig. 3).

Caspase-3 Mediates Proteolytic Activation of PKCδ in Mn-Exposed N27 Cells. PKCδ was recently shown to be one of the important endogenous substrates of caspase-3 (Kikkawa et al., 2002; Brodie and Blumberg, 2003; Kanthasamy et al., 2003). Activated caspase-3 cleaves PKCδ, yielding a 38 kDa regulatory fragment and a 41 kDa catalytic fragment, to persistently increase the kinase activity. Exposure to 300 μM Mn for 24 hr resulted in a dramatic increase in the 41 kDa and 38 kDa catalytic and regulatory PKCδ bands, suggesting that Mn induces PKCδ activation (Fig. 4A). A minimal but not significantly increased level of PKCδ cleavage was observed in untreated cells. Co-treatment with 50 μM Z-DEVD-FMK, a caspase-3 specific inhibitor, almost completely blocked the Mn-induced PKCδ cleavage (Fig. 4B). Densitometric analysis of the 41 kDa PKCδ cleaved bands in Fig 4B revealed that co-treatment with Z-DEVD-FMK results in > 90% reduction in PKCδ cleavage in Mn-treated cells. In addition, exposure to 300 μM Mn did not induce proteolytic cleavage of PKCα (Fig. 4C) or PKCβ (Fig. 4D), suggesting that Mn-induced PKC cleavage is isoform-specific.

Further, exposure to 300 μM Mn increased PKCδ enzymatic kinase activity in parallel with an increase in PKCδ-proteolytically cleaved products (Fig. 5). A 24 hr

treatment with 300 μM Mn induced a 100% increase in PKCδ kinase activity as compared to the control. The kinase activity assay was performed in the absence of lipids to determine the activity due solely to the proteolytically cleaved PKCδ catalytic fragment. The Mn-induced PKCδ kinase activity was completely abolished in cells co-treated with 50 μM Z-DEVD-FMK (caspase-3 inhibitor) or 2 μM rottlerin (PKCδ inhibitor). These results suggest that proteolytic cleavage of PKCδ by caspase-3 increases the kinase activity. Blockade of Mn-induced increases in PKCδ kinase activity by rottlerin further confirms the specificity of PKCδ activation.

Suppression of Mn-Induced DNA Fragmentation by Caspase-3 and PKCδ Inhibitors. We performed a series of experiments to determine whether or not caspase-3-dependent proteolytic activation of PKCδ contributes to Mn-induced apoptosis in dopaminergic cells. Chromatin condensation and DNA fragmentation are hallmarks of apoptosis (Kanthasamy et al., 2003). To quantitatively assess Mn-induced DNA fragmentation, we used an ELISA based Cell Death Detection Plus Kit (Roche Molecular Biochemicals, Indianapolis, IN), as previously described (Anantharam et al., 2002). Mn caused a time-dependent increase in DNA fragmentation (Fig. 6A) as compared to the control. Exposure to 300 μM Mn resulted in a 72% and 209% increase in DNA fragmentation at 12 hr and 24 hr, respectively, as compared to the control. Co-treatment with 50 μM Z-DEVD-FMK blocked Mn-induced DNA fragmentation by 100% and 80% at 12 hr and 24 hr, respectively (Fig. 6A). Furthermore, co-treatment with PKCδ-specific inhibitor rottlerin also blocked Mn-induced DNA fragmentation in a dose-dependent manner (Fig. 6B). Treatment with 1, 3, and 5 μM rottlerin inhibited Mn-induced DNA

fragmentation by 7%, 35%, and 54%, respectively (Fig. 6B), as compared to cells treated with Mn.

Overexpression of Kinase Inactive PKCδ-DN Mutant Rescues Mesencephalic Neuronal Cells from Mn-Induced Apoptosis. In addition to inhibitor studies, we used a genetic approach involving overexpression of a catalytically inactive dominant negative PKCδ^{K376R} (PKCδ-DN) mutant to determine the proapoptotic role of PKCδ in Mn-induced neurotoxicity. We engineered a rat immortalized mesencephalic (N27) cell line to express a dominant negative PKCδ mutant by stably transfecting with plasmids pPKCδ^{K376R}-GFP (in which a lysine at position 376 is mutated to arginine) and pEGFP-N1 (Anantharam et al., 2002). The plasmid pPKCδ^{K376R}-GFP encodes a catalytically inactive PKCδ mutant fused to GFP, and the pEGFP-N1 plasmid encodes the green fluorescent protein alone, which was used as a vector control (Fig. 7A). N27 cells stably expressing the PKCδ-DN-GFP mutant as a fusion protein and vector cells expressing GFP alone are shown in Fig. 7B. Exposure to 300 μM Mn resulted in a 4.5-fold increase in DNA fragmentation in cells expressing GFP-alone (Fig. 7C). However, the response to Mn treatment was significantly attenuated in N27 cells, which stably expressed the PKCδ-DN-GFP mutant. Mn induced 64% less DNA fragmentation in PKCδ-DN-GFP cells compared to cells expressing GFP alone (Fig. 7C). Furthermore, we determined whether manganese still induces cell death despite the blockade of apoptosis in these cells. Measurement of cytotoxicity by MTT assay revealed that Mn-induced cytotoxicity was significantly ($p < 0.01$) reduced in PKCδ-DN-GFP overexpressing cells as compared to GFP-alone-expressing N27 cells (Fig. 7D). 300 μM Mn-exposure decreased the cell

viability by 80% in GFP alone-expressing N27 cells, while the cell viability was decreased by only 30% in PKCδ-DN-GFP overexpressing cells. Together, these results suggest that PKCδ-DN overexpression rescues N27 cells from both Mn-induced cytotoxicity and apoptotic cell death.

Overexpression of Cleavage Resistant Kinase PKCδ ^{D327A}-mutant (PKCδ ^{D327A}-CRM) Protects Mesencephalic Neuronal Cells from Mn-Induced Apoptosis. To further demonstrate that the caspase-3-dependent PKCδ proteolytic cleavage contributes to Mn-induced apoptosis, we used the caspase cleavage site-resistant mutant PKCδ^{D327A} in which aspartate at position 327 is mutated to alanine. N27 cells stably expressing PKCδ^{D327A}-CRM-V5 were generated by using a lentiviral vector tagged with the V5 fusion protein (Fig. 8A & B). LacZ expressing cells were used as a control. As shown Fig. 8C, Mn-induced proteolytic cleavage of endogenous PKCδ was almost completely blocked in PKCδ^{D327A} -CRM mutant overexpressing cells (Fig. 8C). Further, 300 μM Mn failed to induce DNA fragmentation in N27 cells stably overexpressing the PKCδ^{D327A}-CRM mutant, whereas 3 to 4-fold increases in DNA fragmentation were observed in LacZ expressing cells when compared to untreated cells (Fig. 8D). These results strongly suggest that the proteolytic activation of PKCδ mediates Mn-induced apoptosis.

RNAi-Mediated Knockdown of PKCδ Rescues N27 Cells from Mn-Induced Apoptotic Cell Death. To further substantiate the functional role of PKCδ in Mn-induced apoptotic cell death, we examined the effect of PKCδ siRNA on Mn-induced

DNA fragmentation. We recently developed PKCδ siRNAs that specifically suppress PKCδ expression without producing any cytotoxic effect in dopaminergic cells (Yang et al., 2004). In Fig. 9A, *in situ* immunostaining shows a dramatic suppression of PKCδ protein as determined by staining with Alexa 488 in cy3-labeled PKCδ-siRNA transfected cells as compared to non-specific siRNA (siRNA-NS) transfected N27 cells. Furthermore, western blot analysis revealed that the protein levels of PKCδ was suppressed by >60% in PKCδ-siRNA transfected cells (Fig. 9B), whereas PKCδ expression levels were unaltered in siRNA-NS or untreated control cells. Exposure to 300 μM Mn for 24 hr induced 2 to 3-fold increases in DNA fragmentation in siRNA-NS transfected N27 cells and native N27 cells compared to untreated controls. In contrast, Mn-induced DNA fragmentation was completely blocked in PKCδ-siRNA transfected N27 cells (Fig. 9C). Together, these results strongly support a key proapoptotic function of PKCδ in Mn-induced dopaminergic cell death.

DISCUSSION

In the present study, we demonstrate that an inorganic form of Mn can induce apoptosis in mesencephalic dopamine-producing N27 cells through the activation of a series of specific cell death signaling events, including release of cytochrome c from the mitochondria into the cytosol, activation of caspase-3, proteolytic cleavage of PKCδ, and nuclear DNA breakdown. Using a kinase inactive PKCδ^{K376R} dominant negative mutant, a caspase resistant PKCδ^{D327A} mutant, and siRNA against rat PKCδ mRNA, we establish

that PKCδ is a key downstream mediator of Mn-induced apoptosis in dopaminergic neuronal cells.

Mn has been shown to primarily target the nigrostriatal system, including the globus pallidus and substantia nigra (Baek et al., 2003). Mn exposure varies from moderate, as occurs via drinking water and food sources, to high level exposure from occupational and industrial settings such as mining, welding and steel manufacturing (Woolf et al., 2002; Roth and Garrick, 2003; Dobson et al., 2004; Olanow, 2004). Mn can cross the blood-brain-barrier via specific carriers such as transferrin and divalent metal transporter 1 (DMT-1) and also by diffusion (Yokel and Crossgrove, 2004). The normal concentration of manganese in human adult tissues ranges from 3-20 μM (Roth and Garrick, 2003), and the human blood manganese level is 7.2 μg/L (Hauser et al., 1996). Markesbery et al. (1984) reported that the mean brain manganese level is 0.261 μg/g, and Zecca et al. (1994) reported Mn levels in putamen, substantia nigra and neuromelanin of 6.31 ng/mg wet weight, 0.34 ng/mg wet weight, and 58.5 ng/mg wet weight, respectively. Depending on the level of exposure, blood manganese concentrations can increase from 10 to 200-fold (Hauser et al., 1996; Lucchini et al., 1999; Mergler et al., 1999; Woolf et al., 2002; McKinney et al., 2004). Normally, higher relative concentrations of manganese are required in cell culture studies, and the concentrations used in our studies are consistent with other studies (Hirata, 2002; Roth et al., 2002; Stredrick et al., 2004). Still, 300 μM Mn was sufficient to induce apoptotic cell death in N27 cells, as compared to the 1 mM concentration of Mn used in other cell types (Hirata, 2002; Roth et al., 2002). Higher relative concentrations of test compounds are generally needed to elicit responses in cell cultures due to the acute nature of the

treatment period in *in vitro* studies (hours to days) as compared to chronic long-term studies in animal models (days to months). Importantly, the 300 μM manganese concentration used in this study approximates the concentration observed in the striatum of manganese treated rats (Chan et al., 1992; Erikson and Aschner, 2003; Dorman et al., 2004; Gunter et al., 2004). We observed activation of apoptotic signaling molecules, including PKCδ cleavage, at lower manganese concentrations (50 μM) when N27 cells were incubated over a longer period of time (72 hr) (unpublished observations). Thus, the concentration of Mn used in the present study is consistent with the literature and relevant to Mn neurotoxicity.

Recently, we and others demonstrated that both Mn and MMT exposure leads to ROS generation as well as depolarization of the mitochondrial membrane potential in PC12 cells and cortical mitochondrial preparations (Anantharam et al., 2002; Kitazawa et al., 2002). Dopaminergic neurons are particularly vulnerable to oxidative damage (Cantuti-Castelvetri et al., 2003; Dauer and Przedborski, 2003; Dawson and Dawson, 2003). Previously, we observed that dopaminergic cells (PC12) are more vulnerable to MMT-induced ROS generation and apoptotic cell death than non-dopaminergic cells (M212-20) (Kitazawa et al., 2002). We also observed that Trolox (a ROS scavenger), l-deprenyl (an MAO-B inhibitor), or alpha-methyl-p-tyrosine (a tyrosine hydroxylase inhibitor) can effectively attenuate the organic manganese toxicity. Based on these data and available literature, we concluded that excess dopamine in an ROS-rich environment may augment the oxidative insult by formation of highly cytotoxic radicals (Junn and Mouradian, 2001; Kitazawa et al., 2001), which may contribute to the enhanced

susceptibility of dopaminergic neurons to MMT neurotoxicity. In agreement with our results, a recent study demonstrated that manganese is more toxic in catecholamine-producing cells than in non-catecholaminergic cells (Stredrick et al., 2004).

In terms of the neurotoxic effect of manganese on the nigrostriatal system, the effect of manganese on the globus pallidus must be considered since accumulation of manganese is high in this brain region, which is also considered an early target region of manganese neurotoxicity (Roth and Garrick, 2003; Dobson et al., 2004; Olanow, 2004). The prooxidant effect of dopamine may explain the sensitivity of the pallidal neurons to manganese toxicity because of the high dopaminergic innervation to this region from the substantia nigra. The relative sensitivity of nigral neurons as compared to pallidal neurons can not be explained by cell culture models, such as N27 cells, alone. Rather, a detailed temporal and regional analysis of the manganese toxicity response in both the striatum and substantia nigra in animal models is necessary.

Several studies employing cell cultures as well as animal models indicate that caspase-3 plays a major role in the regulation and execution of apoptosis (Kanthasamy et al., 2003). Chronic exposure to inorganic Mn results in a time-dependent activation of caspase-3 in N27 cells. Our data are in agreement with recent reports showing Mn-induced caspase-3 activation in neuronal and non-neuronal cell culture models (Schrantz et al., 1999; Roth et al., 2000a; Chun et al., 2001; Hirata, 2002). However, caspase independent cell death has also been reported following manganese exposure (Roth et al., 2000b; Oubrahim et al., 2001; Stredrick et al., 2004); the different cell types or

methodologies used in these studies may explain the incongruent results. In our study, we did not observe complete protection against Mn-induced cell death with Z-DEVD-FMK and suspect that the concentration of Z-DEVD-FMK (50 μM) was insufficient to completely block Mn-induced cytotoxic cell death. Another possibility is that a minor cell death pathway may be independent of caspase-3. In terms of PD pathogenesis, caspase-3 activation is essential for apoptosis in dopaminergic neurons in human patients with PD as well as in animal models of PD (Hartmann et al., 2000).

We recently established that proteolytic activation of PKCδ by caspase-3 is an important event in the apoptotic cell death of dopaminergic cells (Kanthasamy et al., 2003). In this study, we showed that Mn treatment induces caspase-3-dependent proteolytic cleavage of PKCδ but not of other isoforms including PKCα or PKCβ, suggesting that the cleavage is isoform-specific. Co-treatment with the caspase-3-specific inhibitor Z-DEVD-FMK or overexpression of PKCδ^{D327A}-CRM completely blocked Mn-induced proteolytic cleavage of PKCδ in N27 cells. Recently, we and others have implicated the persistently active catalytic PKCδ fragment in apoptosis in neuronal and non-neuronal cells (Kikkawa et al., 2002; Brodie and Blumberg, 2003; Kanthasamy et al., 2003). Previously, Hirata et al. (2002) showed that Mn treatment induces DNA fragmentation in PC12 cells. We found that Mn exposure induced DNA fragmentation in N27 cells while Z-DEVD-FMK and rottlerin suppressed Mn-induced DNA fragmentation, suggesting that both caspase-3 and PKCδ play a role in Mn-induced apoptosis. The proapoptotic role of PKCδ in Mn-induced neurotoxicity was also confirmed in N27 cells engineered to stably express the catalytically inactive PKCδ

protein (PKCδ^{K376R}-DN). Mn treatment failed to induce DNA fragmentation in N27 cells stably expressing PKCδ-DN, confirming that PKCδ activation is essential for Mn-induced apoptosis. Further, Mn did not induce apoptotic cell death in N27 cells stably expressing the caspase cleavage resistant and catalytically active PKCδ^{D327A}-CRM mutant, confirming the proapoptotic role of cleaved PKCδ.

RNA interference-mediated gene suppression was recently shown to overcome many problems associated with pharmacological inhibitors and antisense oligos, including inherent non-specificity and cytotoxicity (Yang et al., 2004). Because of the high specificity and low toxicity of siRNAs (Yang et al., 2004), we used an siRNA strategy to further confirm the proapoptotic role of PKCδ in Mn-induced apoptotic cell death. We recently demonstrated that siRNA inhibits PKCδ in an isoform-specific manner, which had not been possible with the use of pharmacological inhibitors. Blockade of Mn-induced DNA fragmentation by PKCδ-siRNA in the present study clearly establishes its proapoptotic role in dopaminergic neurodegeneration.

The events downstream of PKCδ activation that lead to apoptotic cell death are still unclear. Recent studies from our lab and others indicate that the catalytically active PKCδ fragment can regulate the activity of a variety of cell signaling molecules associated with apoptotic cell death including scrambalase, DNA-PK, Radd, NFκB, Histone 2B, MAP kinases, Jak2, DIK, Lamin B, Stat3, and others (Kikkawa et al., 2002; Brodie and Blumberg, 2003; Kanthasamy et al., 2003). However, the key downstream

substrate of PKCδ responsible for the Mn-induced apoptotic cell death in dopaminergic neuronal cells has not yet been characterized.

In conclusion, the present study demonstrates that exposure to inorganic Mn induces dopaminergic degeneration by a novel apoptotic pathway mediated by caspase-3-dependent proteolytic activation of PKCδ (Fig.10). This study not only establishes PKCδ as a key downstream mediator of Mn-induced apoptosis but also emphasizes that selective targeting of the proapoptotic kinase PKCδ by siRNA can rescue dopaminergic neurons from Mn-induced dopaminergic degeneration. These findings may also have therapeutic implications in Parkinson's-like diseases.

REFERENCES

Anantharam V, Kitazawa M, Wagner J, Kaul S and Kanthasamy AG (2002) Caspase-3-dependent proteolytic cleavage of protein kinase Cdelta is essential for oxidative stress-mediated dopaminergic cell death after exposure to methylcyclopentadienyl manganese tricarbonyl. *J Neurosci* **22**:1738-1751.

Baek SY, Lee MJ, Jung HS, Kim HJ, Lee CR, Yoo C, Lee JH, Lee H, Yoon CS, Kim YH, Park J, Kim JW, Jeon BS and Kim Y (2003) Effect of manganese exposure on MPTP neurotoxicities. *Neurotoxicology* **24**:657-665.

Brodie C and Blumberg PM (2003) Regulation of cell apoptosis by protein kinase c delta. *Apoptosis* **8**:19-27.

Cantuti-Castelvetri I, Shukitt-Hale B and Joseph JA (2003) Dopamine neurotoxicity: age-dependent behavioral and histological effects. *Neurobiol Aging* **24**:697-706.

Chan AW, Minski MJ, Lim L and Lai JC (1992) Changes in brain regional manganese and magnesium levels during postnatal development: modulations by chronic manganese administration. *Metab Brain Dis* **7**:21-33.

Chun HS, Lee H and Son JH (2001) Manganese induces endoplasmic reticulum (ER) stress and activates multiple caspases in nigral dopaminergic neuronal cells, SN4741. *Neurosci Lett* **316**:5-8.

Dauer W and Przedborski S (2003) Parkinson's disease: mechanisms and models. *Neuron* **39**:889-909.

Dawson TM and Dawson VL (2003) Molecular pathways of neurodegeneration in Parkinson's disease. *Science* **302**:819-822.

Dobson AW, Erikson KM and Aschner M (2004) Manganese neurotoxicity. *Ann N Y Acad Sci* **1012**:115-128.

Dorman DC, McManus BE, Parkinson CU, Manuel CA, McElveen AM and Everitt JI (2004) Nasal toxicity of manganese sulfate and manganese phosphate in young male rats following subchronic (13-week) inhalation exposure. *Inhal Toxicol* **16**:481-488.

Ensing JG (1985) Bazooka: cocaine-base and manganese carbonate [letter]. *J Anal Toxicol* **9**:45-46.

Erikson KM and Aschner M (2003) Manganese neurotoxicity and glutamate-GABA interaction. *Neurochem Int* **43**:475-480.

Gunter TE, Miller LM, Gavin CE, Eliseev R, Salter J, Buntinas L, Alexandrov A, Hammond S and Gunter KK (2004) Determination of the oxidation states of manganese in brain, liver, and heart mitochondria. *J Neurochem* **88**:266-280.

Hartmann A, Hunot S, Michel PP, Muriel MP, Vyas S, Faucheux BA, Mouatt-Prigent A, Turmel H, Srinivasan A, Ruberg M, Evan GI, Agid Y and Hirsch EC (2000) Caspase-3: A vulnerability factor and final effector in apoptotic death of dopaminergic neurons in Parkinson's disease. *Proc Natl Acad Sci U S A* **97**:2875-2880.

Hauser RA, Zesiewicz TA, Martinez C, Rosemurgy AS and Olanow CW (1996) Blood manganese correlates with brain magnetic resonance imaging changes in patients with liver disease. *Can J Neurol Sci* **23**:95-98.

Hirata Y (2002) Manganese-induced apoptosis in PC12 cells. *Neurotoxicol Teratol* **24**:639.

Jenner P (2003) Oxidative stress in Parkinson's disease. *Ann Neurol* **53 Suppl 3**:S26-36; discussion S36-28.

Junn E and Mouradian MM (2001) Apoptotic signaling in dopamine-induced cell death: the role of oxidative stress, p38 mitogen-activated protein kinase, cytochrome c and caspases. *J Neurochem* **78**:374-383.

Kanthasamy AG, Kitazawa M, Kanthasamy A and Anantharam V (2003) Role of proteolytic activation of protein kinase Cdelta in oxidative stress-induced apoptosis. *Antioxid Redox Signal* **5**:609-620.

Kaul S, Kanthasamy A, Kitazawa M, Anantharam V and Kanthasamy AG (2003) Caspase-3 dependent proteolytic activation of protein kinase C delta mediates and regulates 1-methyl-4-phenylpyridinium (MPP+)-induced apoptotic cell death in dopaminergic cells: relevance to oxidative stress in dopaminergic degeneration. *Eur J Neurosci* **18**:1387-1401.

Kikkawa U, Matsuzaki H and Yamamoto T (2002) Protein Kinase Cdelta (PKCdelta): Activation Mechanisms and Functions. *J Biochem (Tokyo)* **132**:831-839.

Kitazawa M, Anantharam V and Kanthasamy AG (2001) Dieldrin-induced oxidative stress and neurochemical changes contribute to apoptopic cell death in dopaminergic cells. *Free Radic Biol Med* **31**:1473-1485.

Kitazawa M, Anantharam V and Kanthasamy AG (2003) Dieldrin induces apoptosis by promoting caspase-3-dependent proteolytic cleavage of protein kinase Cdelta in dopaminergic cells: relevance to oxidative stress and dopaminergic degeneration. *Neuroscience* **119**:945-964.

Kitazawa M, Wagner JR, Kirby ML, Anantharam V and Kanthasamy AG (2002) Oxidative stress and mitochondrial-mediated apoptosis in dopaminergic cells exposed to methylcyclopentadienyl manganese tricarbonyl. *J Pharmacol Exp Ther* **302**:26-35.

Lucchini R, Apostoli P, Perrone C, Placidi D, Albini E, Migliorati P, Mergler D, Sassine MP, Palmi S and Alessio L (1999) Long-term exposure to "low levels" of manganese oxides and neurofunctional changes in ferroalloy workers. *Neurotoxicology* **20**:287-297.

Markesbery WR, Ehmann WD, Hossain TI and Alauddin M (1984) Brain manganese concentrations in human aging and Alzheimer's disease. *Neurotoxicology* **5**:49-57.

McKinney AM, Filice RW, Teksam M, Casey S, Truwit C, Clark HB, Woon C and Liu HY (2004) Diffusion abnormalities of the globi pallidi in manganese neurotoxicity. *Neuroradiology* **46**:291-295.

Mergler D, Baldwin M, Belanger S, Larribe F, Beuter A, Bowler R, Panisset M, Edwards R, de Geoffroy A, Sassine MP and Hudnell K (1999) Manganese neurotoxicity, a continuum of dysfunction: results from a community based study. *Neurotoxicology* **20**:327-342.

Olanow CW (2004) Manganese-induced parkinsonism and Parkinson's disease. *Ann N Y Acad Sci* **1012**:209-223.

Oubrahim H, Stadtman ER and Chock PB (2001) Mitochondria play no roles in Mn(II)-induced apoptosis in HeLa cells. *Proc Natl Acad Sci U S A* **98**:9505-9510.

Roth JA, Feng L, Walowitz J and Browne RW (2000a) Manganese-induced rat pheochromocytoma (PC12) cell death is independent of caspase activation. *J. Neurosci. Res.* **61**:162-171.

Roth JA, Feng L, Walowitz J and Browne RW (2000b) Manganese-induced rat pheochromocytoma (PC12) cell death is independent of caspase activation [In Process Citation]. *J Neurosci Res* **61**:162-171.

Roth JA and Garrick MD (2003) Iron interactions and other biological reactions mediating the physiological and toxic actions of manganese. *Biochem Pharmacol* **66**:1-13.

Roth JA, Horbinski C, Higgins D, Lein P and Garrick MD (2002) Mechanisms of manganese-induced rat pheochromocytoma (PC12) cell death and cell differentiation. *Neurotoxicology* **23**:147-157.

Schrantz N, Blanchard DA, Mitenne F, Auffredou MT, Vazquez A and Leca G (1999) Manganese induces apoptosis of human B cells: caspase-dependent cell death blocked by bcl-2. *Cell Death Differ.* **6**:445-453.

Stredrick DL, Stokes AH, Worst TJ, Freeman WM, Johnson EA, Lash LH, Aschner M and Vrana KE (2004) Manganese-induced cytotoxicity in dopamine-producing cells. *Neurotoxicology* **25**:543-553.

Woolf A, Wright R, Amarasiriwardena C and Bellinger D (2002) A child with chronic manganese exposure from drinking water. *Environ Health Perspect* **110**:613-616.

Yang Y, Kaul S, Zhang D, Anantharam V and Kanthasamy AG (2004) Suppression of caspase-3-dependent proteolytic activation of protein kinase C delta by small

interfering RNA prevents MPP+-induced dopaminergic degeneration. *Mol Cell Neurosci* **25**:406-421.

Yokel RA and Crossgrove JS (2004) Manganese toxicokinetics at the blood-brain barrier. *Res Rep Health Eff Inst*:7-58; discussion 59-73.

Zecca L, Pietra R, Goj C, Mecacci C, Radice D and Sabbioni E (1994) Iron and other metals in neuromelanin, substantia nigra, and putamen of human brain. *J Neurochem* **62**:1097-1101.

FOOTNOTES

This study was supported by the National Institute of Health (NIH) grants ES 10586, NS 38644 and NS 45133.

*Address correspondence to:
Dr. Anumantha G. Kanthasamy, Parkinson's Disorder Research Program
Department of Biomedical Sciences, Iowa State University, 2062 College of Veterinary Medicine Building, Ames, IA 50011-1250 U.S.A. Phone: (515) 294-2516
Fax: (515) 294-2315, e-mail: akanthas@iastate.edu

FIGURE LEGENDS

Fig.1. Caspase-3-mediated Mn-induced cytotoxicity in N27 mesencephalic neuronal cells. A, MTT cytotoxicity assay; N27 cells were treated with 10 μM to 5 mM $MnCl_2$ for 24 hr and assayed for cell death using MTT (3-4,5-Dimethylthiazol-3-yl)-2,5-diphenyl tetrazolium bromide). Data represent results from six to eight individual measurements and are expressed as mean ± SEM. B, Sytox-green cytotoxicity assay; Mn-induced changes in cell death measured 24 hr after exposure to 100 μM or 300 μM $MnCl_2$ in the presence or absence of a caspase-3 inhibitor, Z-DEVD-FMK (50 μM). Data represent results from eight separate measurements and are expressed as mean ± SEM. *$p<0.05$ as compared to control group.

Fig. 2. Release of cytochrome c in Mn-treated N27 cells. Subconfluent cultures of N27 cells were treated with 300 μM $MnCl_2$ for 6 hr and 12 hr, cytosolic fractions were isolated, and cytochrome c was measured by ELISA. The values are expressed as mean ± SEM from six individual measurements and *$p<0.05$ was considered significant compared to control groups.

Fig. 3. Activation of caspase-3 in Mn-treated N27 cells. Subconfluent cultures of N27 cells were treated with Mn (100 μM and 300 μM) for 12 hr and 24 hr. The enzyme activity was assayed using a caspase-3 substrate. The values are expressed as mean ± SEM from six individual measurements and *$p<0.05$ was considered significant compared to the control.

Fig. 4. Caspase-3-dependent proteolytic cleavage of PKCδ in Mn-induced neurotoxicity. A, PKCδ immunoblot after Mn treatment. N27 cells were treated with either 100 μM or 300 μM Mn for 24 hr and proteins were separated by 10% SDS-PAGE and probed with PKCδ antibody to observe both native (72-74 kDa) and cleaved (38-41 kDa) PKCδ bands. B, Effect of caspase-3 inhibitor on Mn-induced PKCδ cleavage. N27 cells were treated with 300 μM Mn with or without the addition of 50 μM Z-DEVD-FMK for 24 hr and then a PKCδ immunoblot was performed as described above. To confirm equal protein loading in each lane, the membranes were reprobed with β-actin antibody. (C & D) PKCα and PKCβ1 immunoblot after Mn treatment. N27 cells were treated with 100 μM or 300 μM Mn for 24 hr and probed with either PKCα or PKCβ1.

Fig. 5. Mn-induced PKCδ cleavage increases the kinase activity. Subconfluent cultures of N27 cells were harvested at 24 hr after treatment with 300 μM Mn in the presence or absence of 50 μM Z-DEVD-FMK (caspase-3 inhibitor) or 2 μM rottlerin (PKCδ inhibitor). Cell lysates were isolated and PKCδ was immunoprecipitated from treated cell lysate and the enzyme activity was measured by ^{32}P phosphorylation. The values are expressed as a percentage of control cells, and *$p<0.05$ was considered significant when comparing Mn-treated cells to other treatment groups.

Fig. 6. Mn-induced apoptosis in N27 cells. A, Effect of the caspase-3 inhibitor Z-DEVD-FMK on Mn-induced DNA fragmentation in N27 cells. Subconfluent cultures of N27 cells were harvested at 12 hr and 24 hr after treatment with 300 μM Mn in the presence or absence of 50 μM Z-DEVD-FMK. DNA fragmentation was quantified using

ELISA. The data are expressed as percentage of DNA fragmentation compared to untreated control cells, and asterisks (*$p<0.05$, **$p<0.01$) indicate significant differences compared to control cells. B, Effect of rottlerin on Mn-induced DNA fragmentation in N27 cells. N27 cells were treated with 300 μM Mn for 24 hr with or without 1, 3, or 5 μM rottlerin. DNA fragmentation was reduced by rottlerin in N27 cells in a dose-dependent manner. The data are expressed as percentage of DNA fragmentation observed in Mn-treated cells. The data represent the mean ± SEM of six individual measurements. Asterisks (**$p<0.01$) indicate significant differences between Mn-treated cells and Mn plus rottlerin-treated cells.

Fig. 7. Overexpression of catalytically inactive PKCδ^{K376R} protein (PKCδ-DN) attenuates Mn-induced apoptosis. A, Schematic of plasmid constructs. pEGFP-NI construct encodes the green fluorescent protein (GFP) mRNA transcribed under the 5' human cytomegalovirus (CMV) immediate early promoter, and the mRNA is stabilized with the 3' SV40 mRNA polyadenylation signal (pA) and was used as a vector control. The PKCδ^{K376R}-GFP (PKCδ-DN-GFP) construct encodes the kinase inactive PKCδ-GFP fusion transcript. B, Fluorescent images showing the stable expression of both the GFP control vector (left panel) and PKCδ-DN-GFP fusion protein (right panel) in N27 cells (200 X magnification). C, DNA fragmentation assay and D, Cell viability assay. Subconfluent cultures of N27 cells stably expressing the vector or PKCδ-DN-GFP fusion protein were treated with 100 μM or 300 μM Mn for 24 hr. Cell viability and DNA fragmentation was assayed using MTT and ELISA, respectively as described in the methods section. The data are expressed as percentage of apoptosis observed in control

cells. The data represent mean ± SEM of four to six individual measurements. Single asterisks (*p<0.05) indicate significant differences when compared to untreated control, and double asterisks (**p<0.01) indicate a significant difference between the 300 μM Mn-treated PKCδ-DN-GFP mutant cells and the 300 μM Mn-treated vector cells expressing GFP alone.

Fig. 8. Overexpression of cleavage-resistant PKCδ^{D327A} protein (PKCδ-CRM) attenuates Mn-induced apoptosis. A, Schematic of plasmid constructs. PKCδ-CRM-V5 construct encodes cleavage resistant mutant of PKCδ-CRM-V5 tag transcript mRNA transcribed under the 5' human cytomegalovirus (CMV) immediate early promoter, and the mRNA is stabilized with the 3' SV40 mRNA polyadenylation signal (pA). B, Fluorescent images showing the stable expression of V5 tag in N27 cells expressing the PKCδ-CRM-V5 tag (200 X magnification). C, PKCδ-CRM prevents Mn-induced PKCδ cleavage. Subconfluent cultures of N27 cells stably expressing the vector or PKCδ-CRM-V5 protein were treated with 300 μM Mn for 24 hr. LacZ expressing cells were used as a vector control. PKCδ cleavage was determined by Western blot. D, DNA fragmentation assay. Subconfluent cultures of N27 cells stably expressing the vector or PKCδ-CRM-V5 protein were treated with 300 μM Mn for 24 hr and then DNA fragmentation was measured by ELISA. The data represent mean ± SEM of four to six individual measurements. Single asterisk (*p<0.01) indicates a significant difference between the 300 μM Mn-treated PKCδ-CRM-V5 mutant cells and the 300 μM Mn-treated LacZ vector control cells.

Fig. 9. Suppression of PKCδ by siRNA rescues N27 cells from Mn-induced apoptotic cell death. A, PKCδ-siRNA suppresses PKCδ protein expression. Cells were transfected with cy3-labeled PKCδ-siRNA (25 nM) or cy3-labeled non-specific (NS)-siRNA and PKCδ expression was observed following immunostaining using anti-PKCδ antibody and Alexa-488 secondary antibody. The nuclei were visualized by Hoechst 33342 counterstaining. Merged images show expression of PKCδ (green), cy-3-labeled PKCδ-siRNA or siRNA-NS (red), and nuclear staining (blue). Cells were observed under a Nikon inverted fluorescence microscope and pictures were captured with a SPOT digital camera (Diagnostic Instruments, Sterling Heights, MI). PKCδ-siRNA markedly reduced PKCδ expression, whereas cells transfected with cy3-labeled siRNA-NS (25 nM) show normal PKCδ expression. B, Western blot analysis of PKCδ expression at 24 hr post-transfection with PKCδ-siRNA. Membranes were reprobed with β-actin (43 kDa) antibody to confirm equal protein loading. C, PKCδ-siRNA completely protects N27 cells against Mn-induced DNA fragmentation. Subconfluent cultures of N27 cells were transfected with siRNA-δ-4 (25 nM) or non-specific siRNA (siRNA-NS) for 24 hr and then the cells were treated with 300 μM Mn for an additional 24 hr. After exposure to Mn, DNA fragmentation was measured. Untransfected N27 cells not exposed to Mn were used as controls. The data represent the mean $\pm$ SEM from six individual measurements.

Fig. 10. A proposed model describing the sequence of cell death signaling events in Mn-induced apoptosis. (1) Mn treatment impairs mitochondrial function, resulting in cytochrome c release into the cytosol; (2) cytosolic cytochrome c activates caspase

cascade (3) caspase-3 mediates proteolytic cleavage of PKCδ; proteolytically activated PKCδ mediates DNA fragmentation (4) and apoptosis (5). Effect of pharmacological inhibitors and genetic modulators on Mn-induced apoptosis. (a) Co-treatment with caspase-3 specific inhibitor Z-DEVD-FMK prevents proteolytic activation of PKCδ and Mn-induced DNA fragmentation. (b) Co-treatment with PKCδ specific inhibitor rottlerin attenuates Mn-induced DNA fragmentation. (c) Overexpression of PKCδ^{D327A}-CRM mutant protein significantly attenuates caspase-3-mediated PKCδ cleavage and DNA fragmentation; (d) overexpression of dominant negative mutant PKCδ^{K376R}-DN almost completely suppresses Mn-induced DNA fragmentation; and (e) RNAi mediated knockdown of PKCδ with siRNA-PKCδ rescues N27 cells from Mn-induced apoptotic cell death.

JPET Fast Forward. Published on December 17, 2004 as DOI: 10.1124/jpet.104.078469
This article has not been copyedited and formatted. The final version may differ from this version.

Fig. 1

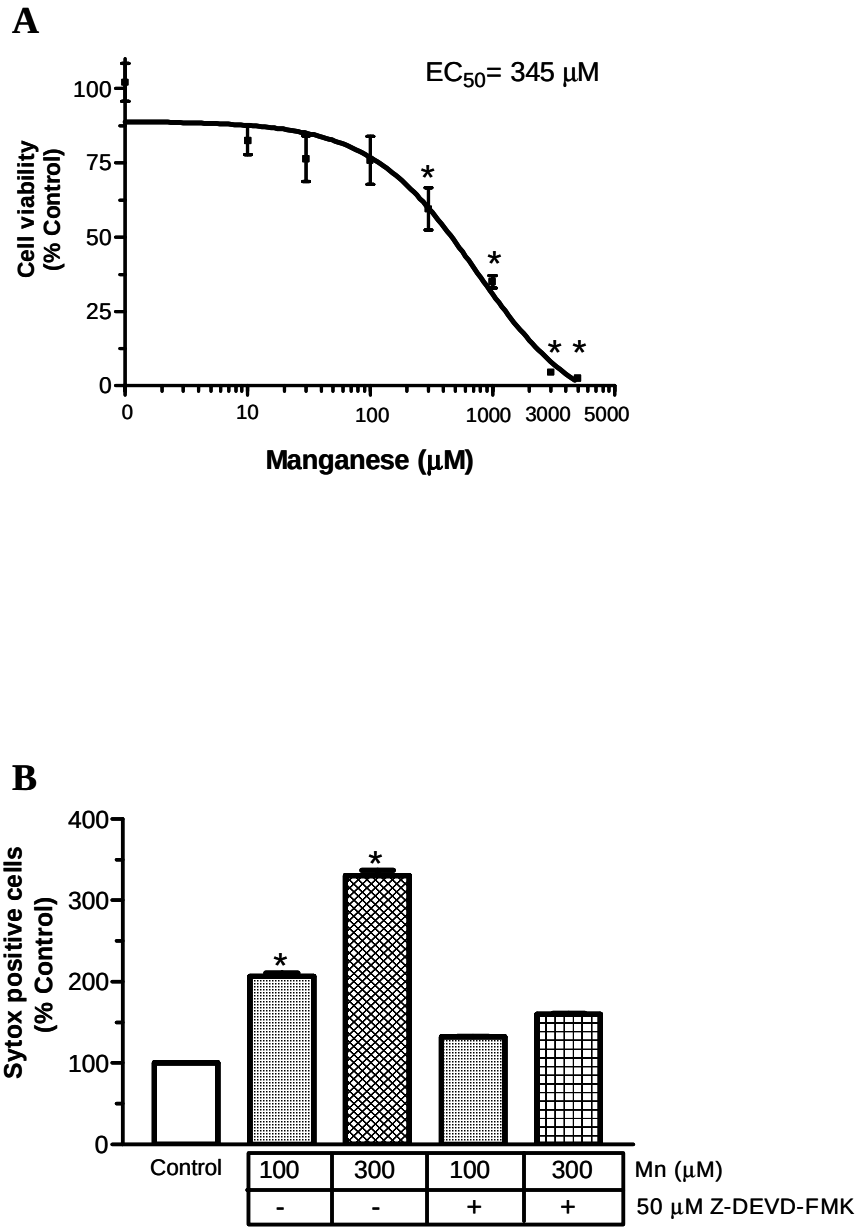

JPET Fast Forward. Published on December 17, 2004 as DOI: 10.1124/jpet.104.078469
This article has not been copyedited and formatted. The final version may differ from this version.

Fig. 2

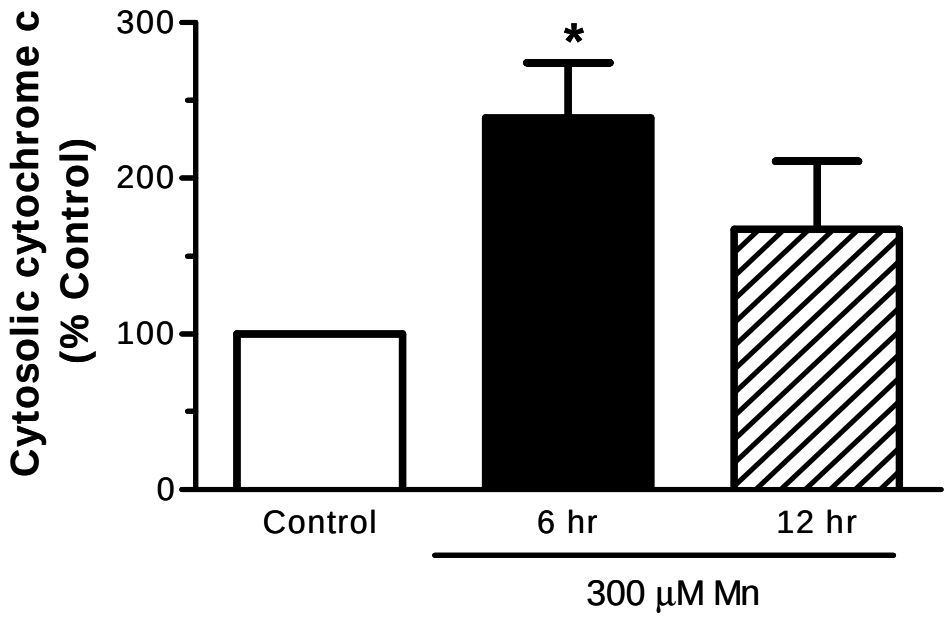

JPET Fast Forward. Published on December 17, 2004 as DOI: 10.1124/jpet.104.078469
This article has not been copyedited and formatted. The final version may differ from this version.

Fig. 3

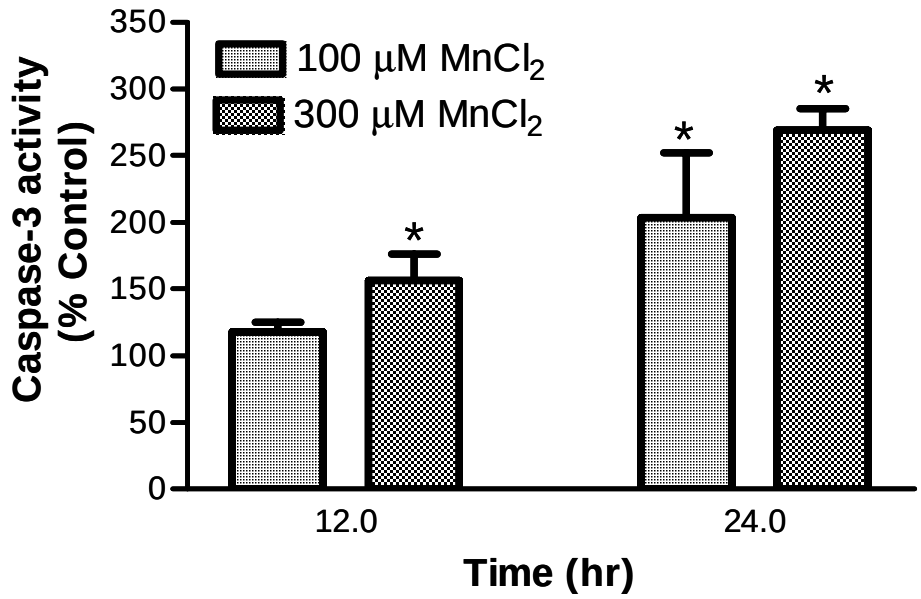

JPET Fast Forward. Published on December 17, 2004 as DOI: 10.1124/jpet.104.078469
This article has not been copyedited and formatted. The final version may differ from this version.

Fig. 4

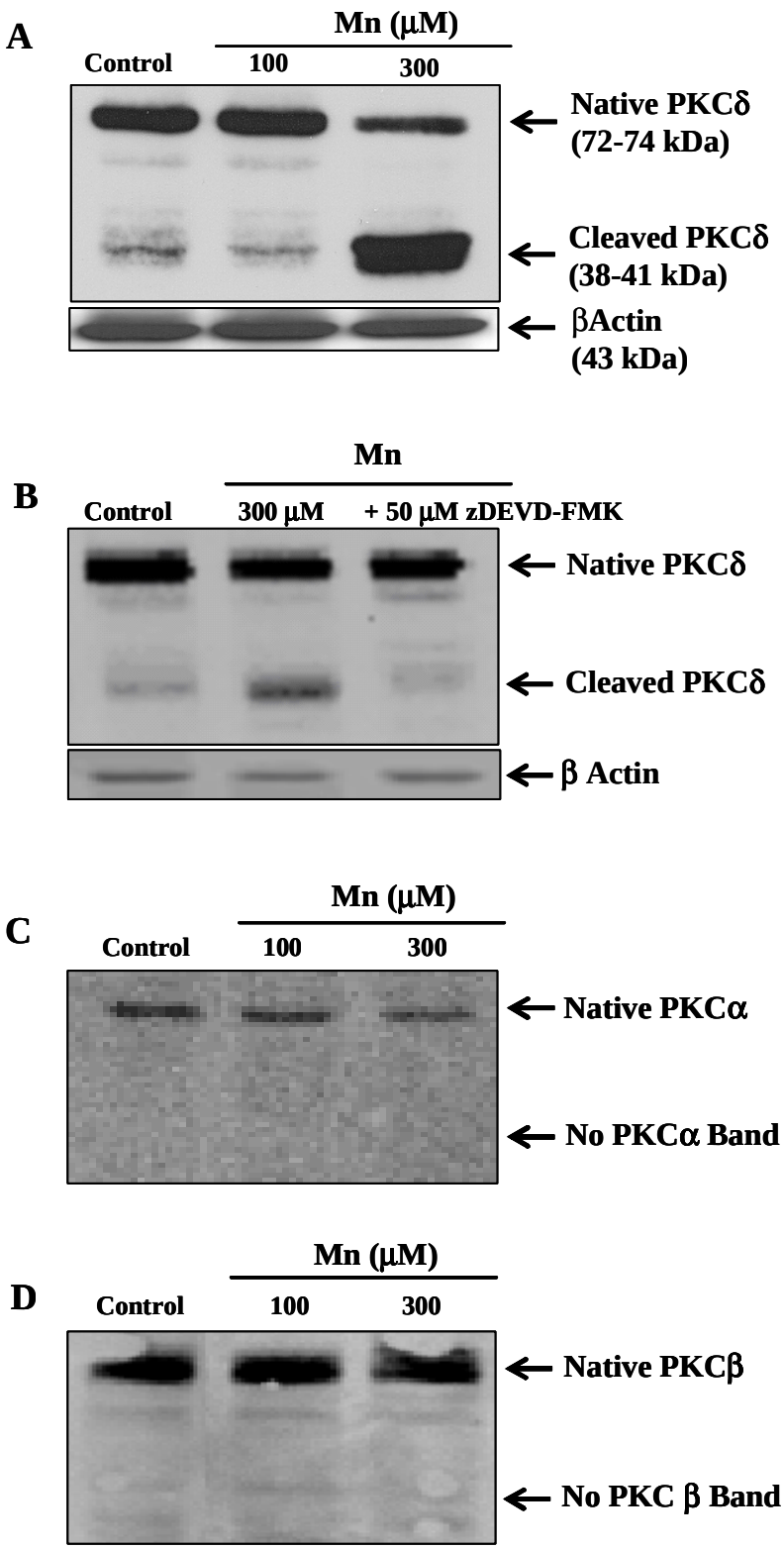

JPET Fast Forward. Published on December 17, 2004 as DOI: 10.1124/jpet.104.078469
This article has not been copyedited and formatted. The final version may differ from this version.

Fig. 5

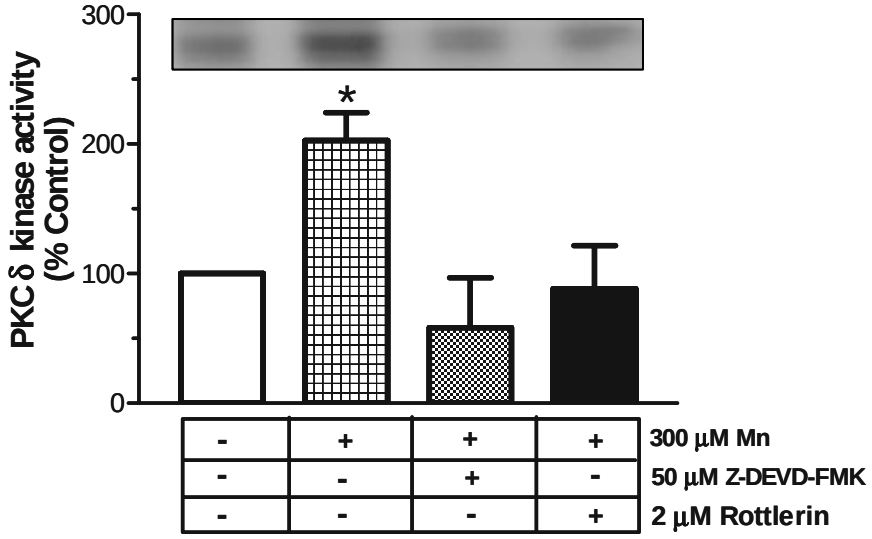

JPET Fast Forward. Published on December 17, 2004 as DOI: 10.1124/jpet.104.078469
This article has not been copyedited and formatted. The final version may differ from this version.

Fig. 6

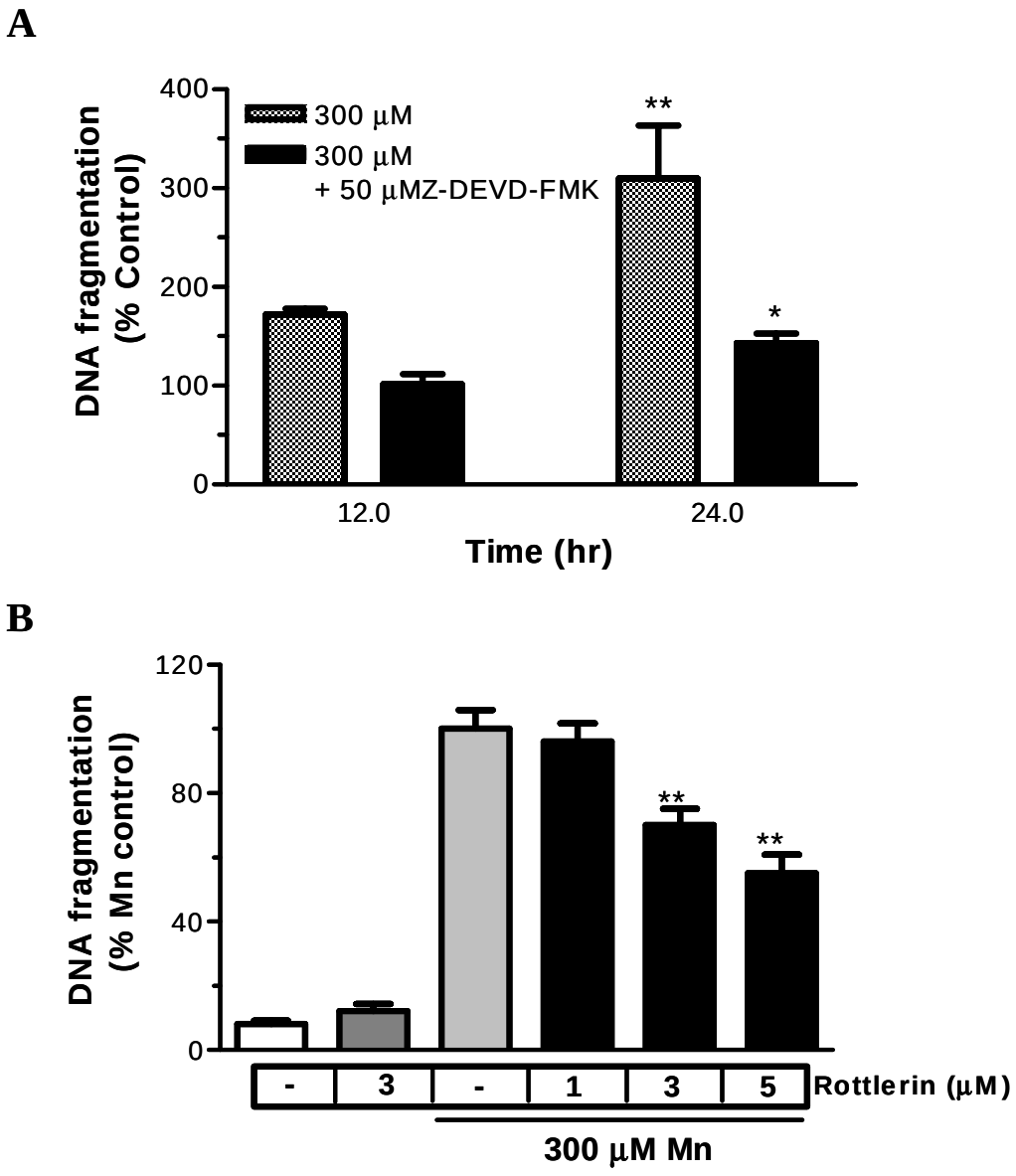

JPET Fast Forward. Published on December 17, 2004 as DOI: 10.1124/jpet.104.078469
This article has not been copyedited and formatted. The final version may differ from this version.

Fig. 7

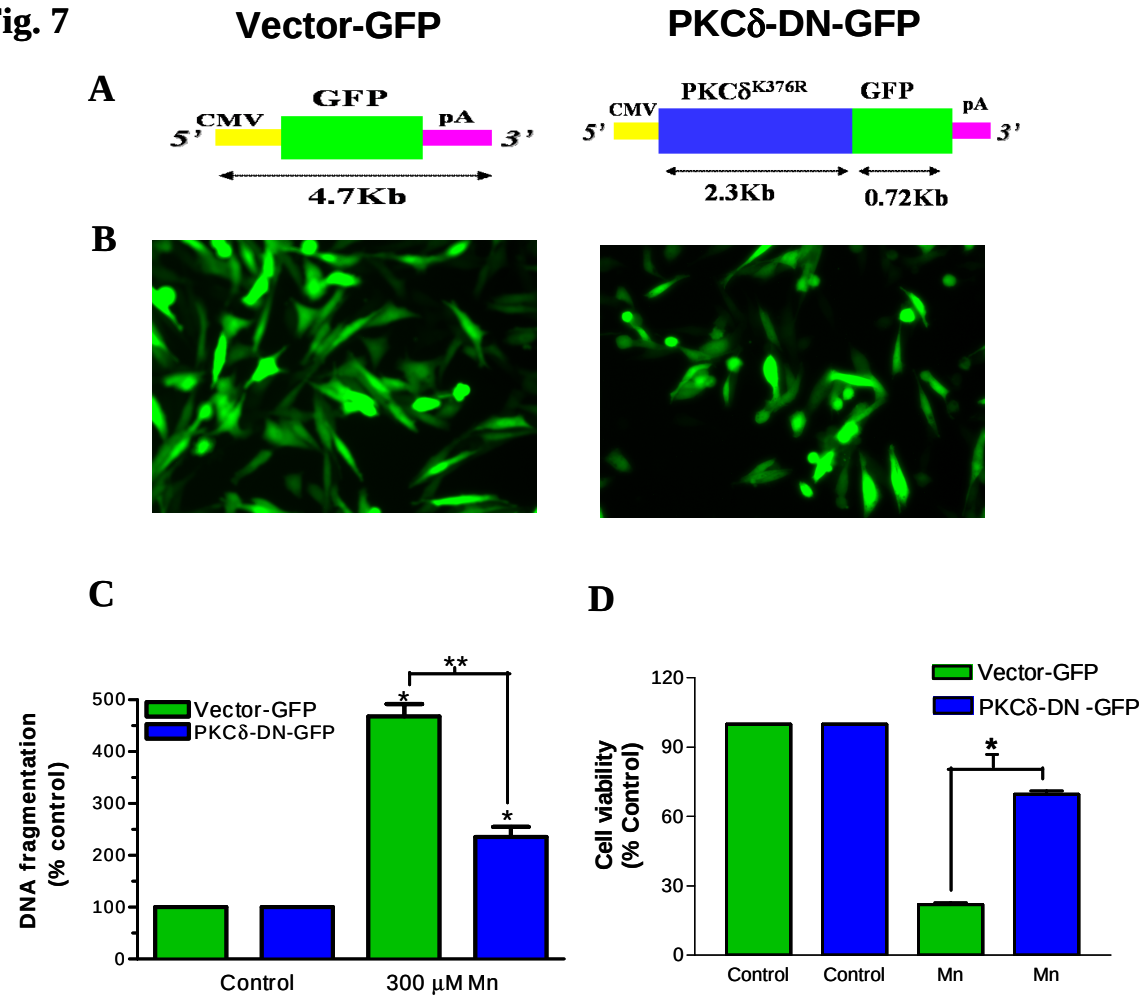

JPET Fast Forward. Published on December 17, 2004 as DOI: 10.1124/jpet.104.078469
This article has not been copyedited and formatted. The final version may differ from this version.

Fig. 8

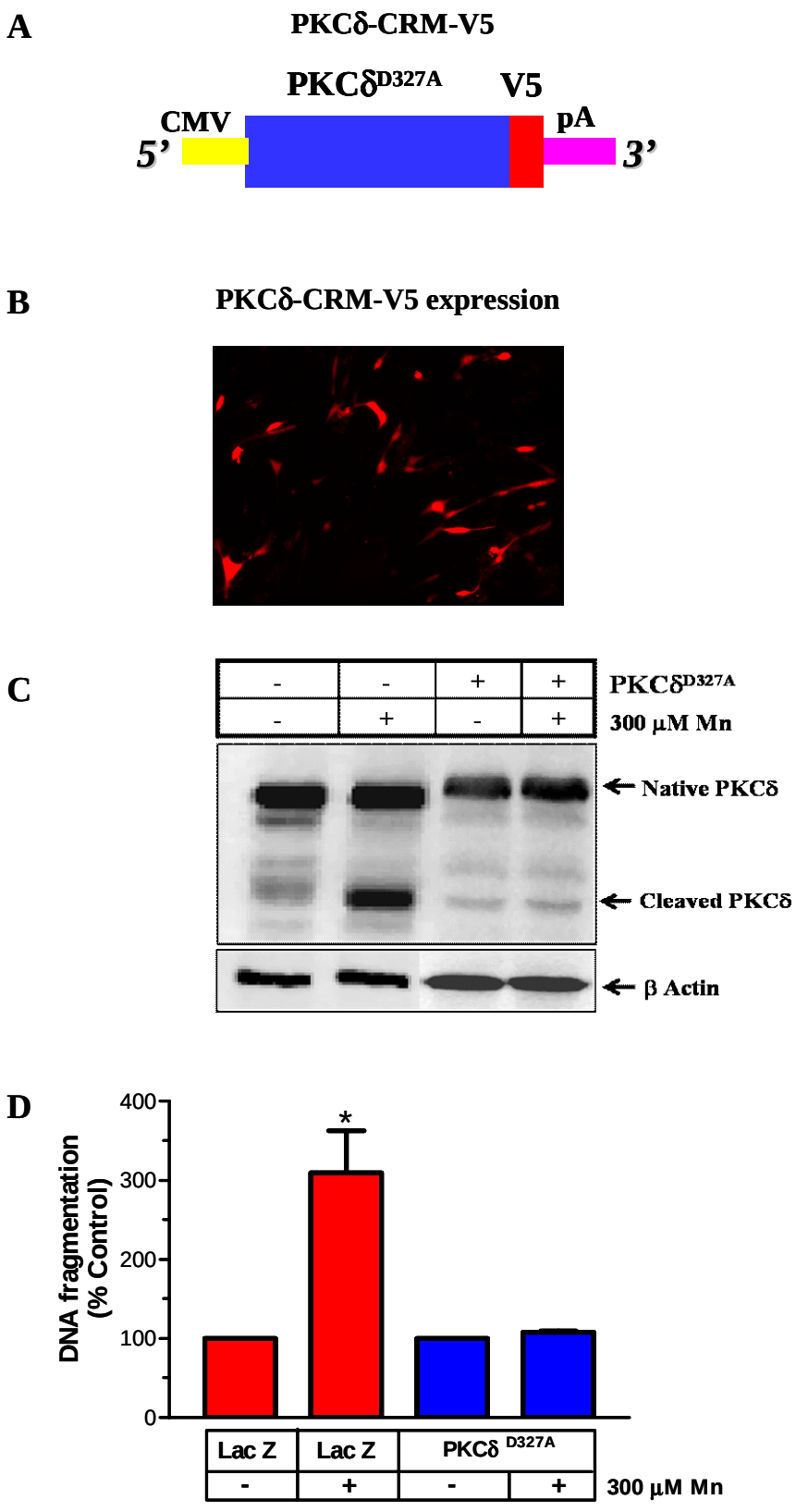

JPET Fast Forward. Published on December 17, 2004 as DOI: 10.1124/jpet.104.078469
This article has not been copyedited and formatted. The final version may differ from this version.

Fig. 9

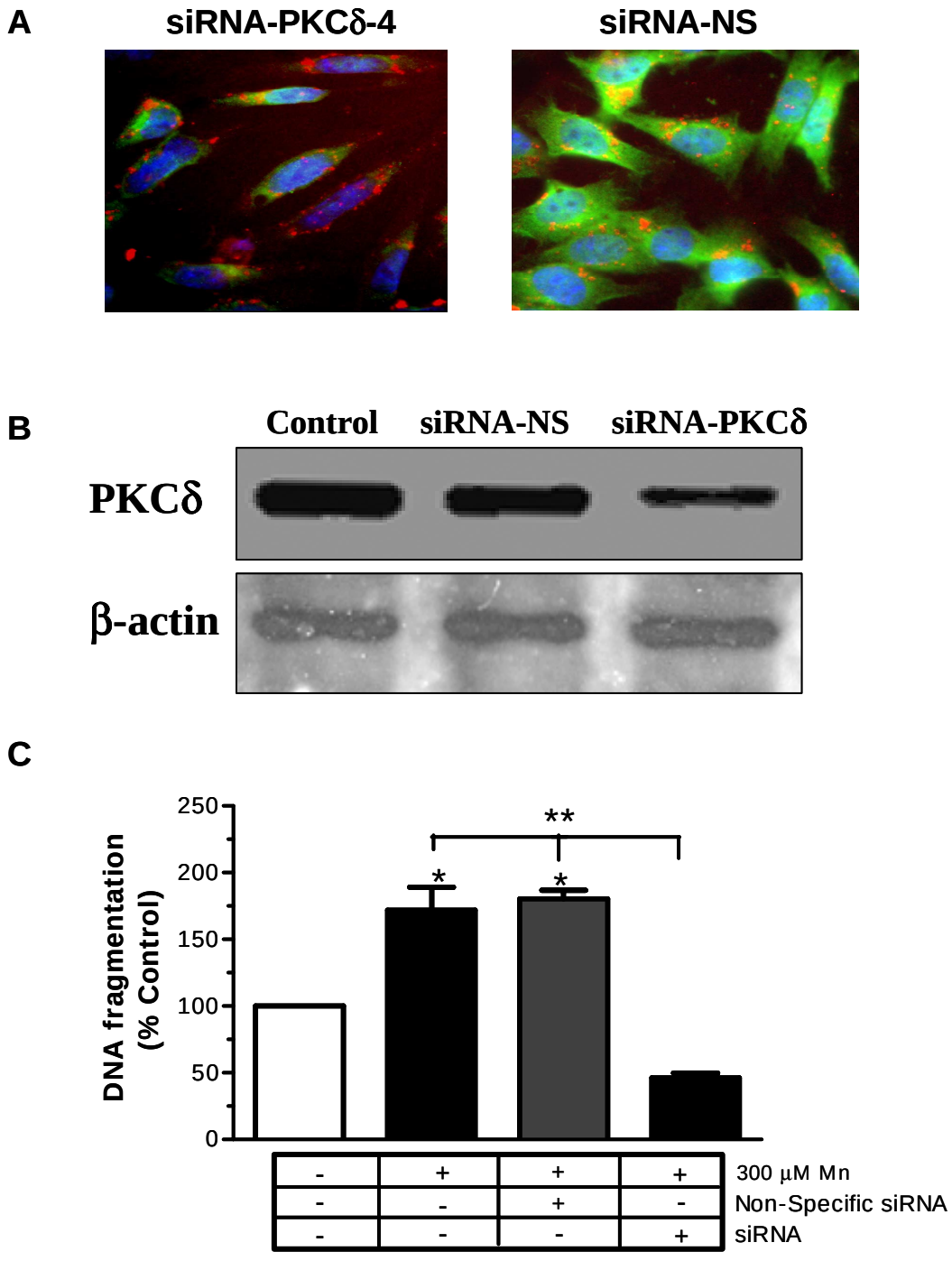

JPET Fast Forward. Published on December 17, 2004 as DOI: 10.1124/jpet.104.078469
This article has not been copyedited and formatted. The final version may differ from this version.

Fig. 10